ELSEVIER

Spectrochimica Acta Part B 52 (1997) 553–565

SPECTROCHIMICA ACTA PART B

Comparison of argon and neon as discharge gases in a direct-current glow discharge A mathematical simulation

A. Bogaerts*, R. Gijbels

Department of Chemistry, University of Antwerp (UIA), Universiteitsplein 1, B-2610 Wilrijk, Belgium

Received 27 September 1996; accepted 21 November 1996

Abstract

A number of three-dimensional models (Monte Carlo and fluid models) for the different plasma species in a glow discharge were developed earlier and were combined in order to obtain an overall picture of the direct-current glow discharge in argon. In the present work, these models are applied to a neon discharge, and a comparison is made between these two discharge gases with respect to the pressure–current–voltage characteristics, the densities and energies of the plasma species, the electric field and potential distributions, the erosion rates at the cathode, and the relative importance of certain plasma processes (i.e., in the creation of gas metastable atoms, the ionization of sputtered atoms and the sputtering process). © 1997 Elsevier Science B.V.

Keywords: Glow discharge; Mathematical modelling; Discharge gas; Argon; Neon

1. Introduction

Glow discharges are used as analytical sources for mass spectrometry, optical emission, absorption and fluorescence spectrometry [1], as etching and deposition devices, e.g. in the microelectronics industry [2] and also as metal ion lasers [3]. Glow discharges employed in analytical chemistry are mostly operated with argon as the discharge gas. Some papers, however, also report the use of neon as the working gas in a glow discharge (see, for example, [4–13]), for example to eliminate specific molecular interferences in the mass spectrum [8,13]. It is generally known [8,10,12] that the gas pressure in a neon discharge must be higher in comparison to an argon discharge in order to achieve comparable current–voltage values, but that both gases exhibit similar analytical performances.

In earlier work, we have developed a set of mathematical models to calculate explicitly the behaviour of the plasma particles in a direct-current glow discharge in argon, in order to obtain an overall picture of the discharge [14–23]. In the present paper, these mathematical models have been applied to neon as the discharge gas, and a comparison is made between argon and neon, to understand better the differences and similarities of these two discharge gases.

2. Description of the modelling work

The models have been described in detail for argon in [14–23]. In this paper, only a short outline is given. The plasma species considered are the gas (argon or

* Corresponding author.

PII S0584-8547(96)01658-8

neon) atoms at rest, uniformly distributed throughout the discharge, singly charged positive gas ions, fast gas atoms, metastable gas atoms, electrons (subdivided in a fast and a slow group) and sputtered analyte atoms and the corresponding ions (copper was taken as an example). These species are described with Monte Carlo and fluid models.

The fast electrons are simulated by a Monte Carlo model [14–16]; collision processes taken into account are elastic collisions with gas atoms, electron impact excitation and ionization from the gas atom ground state and from the gas atom metastable levels, and ionization of sputtered copper atoms. The slow electrons are described, together with the gas ions, in a fluid approach [15,16], based on continuity and transport equations (diffusion and migration); these are coupled to the Poisson equation to achieve a self-consistent electric field distribution. The gas

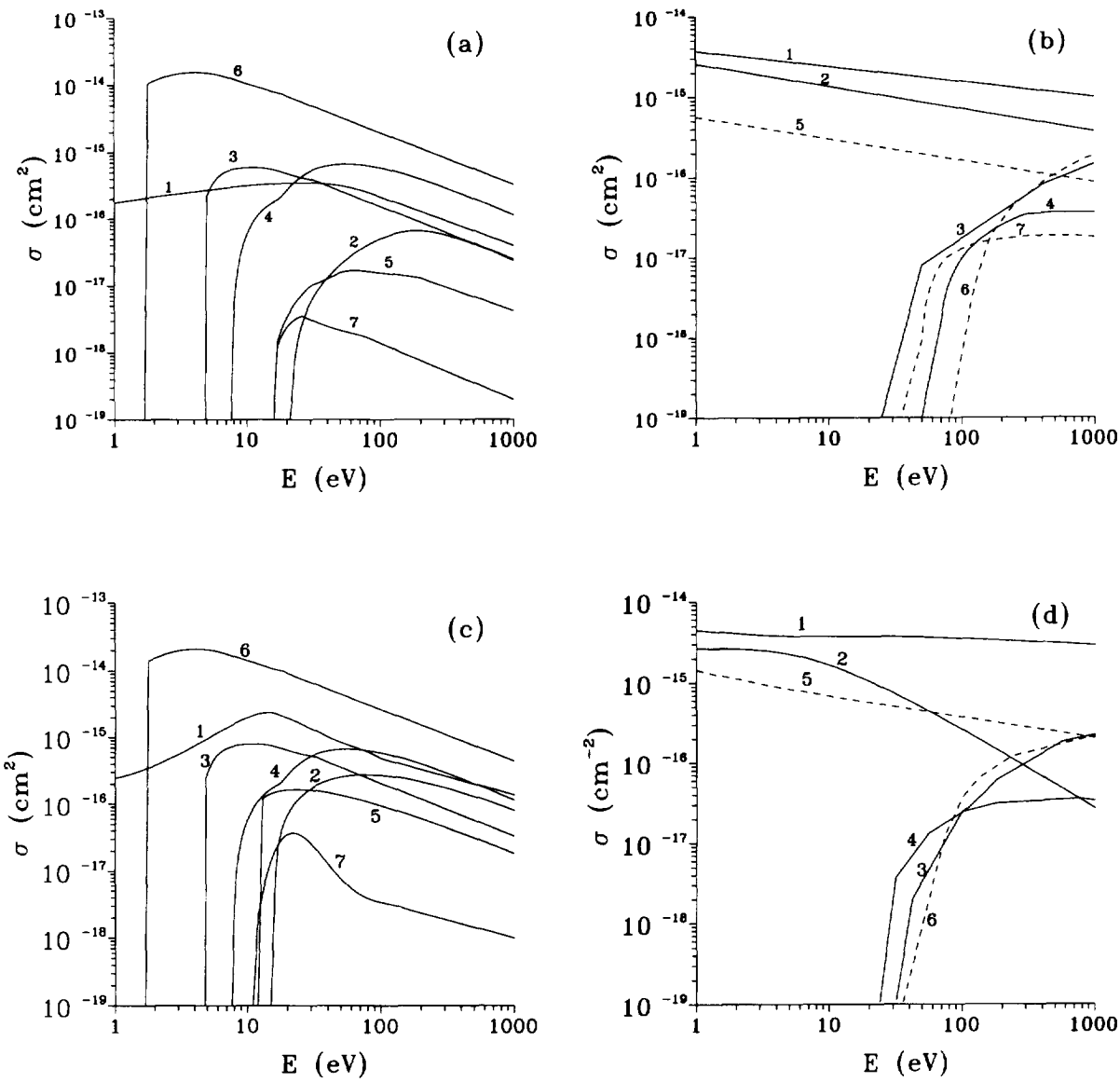

ions are also simulated with a Monte Carlo model in the cathode dark space (CDS), together with the fast gas atoms which are created from the ions by symmetric charge transfer and elastic collisions [14,16,17]; collision processes incorporated in this model comprise symmetric charge transfer (for the ions) and elastic collisions with gas atoms, ion and atom impact ionization and excitation of gas atoms (for the ions and atoms). The behaviour of the metastable atoms is described by a fluid model, based on a balance equation incorporating all known production and loss processes [18,19]; the production processes include electron, gas ion and atom impact excitation, and gas ion–electron radiative recombination, whereas the loss processes comprise electron impact ionization and excitation from the metastable level, electron collisional transfer to nearby energy levels, metastable atom–metastable atom collisions, Penning ionization of sputtered copper atoms, two-body and three-body collisions with ground state gas atoms, and diffusion and subsequent deexcitation at the walls. The thermalization of the sputtered copper atoms is simulated by a Monte Carlo model [20]. The further transport of the copper atoms (diffusion dominated), their ionization, and the transport of the created ions (by diffusion and migration in the electric field) are described with a fluid model [19,21]; the ionization processes considered in this model are Penning ionization by gas metastables, asymmetric charge transfer by gas ions, and electron impact ionization. Finally, the copper ions are also simulated in the CDS by a Monte Carlo model [19,21]. All these models are coupled to each other into a comprehensive modelling network, through the interaction processes between the plasma particles, and they are solved iteratively until final convergence is reached.

The models are applied to the standard cell for analysing flat samples in the VG9000 glow discharge mass spectrometer (VG Elemental, Thermo Instruments). The Monte Carlo models are developed in three dimensions, whereas the fluid models are solved in two dimensions, since the three dimensions can be reduced to two dimensions because of the cylindrical symmetry of the cell. This modelling network originally developed for argon, can also be applied to neon, if the corresponding input data (cross sections etc.) for neon are introduced.

Fig. 1a presents the cross sections for electron collisions in the neon discharge as a function of electron energy. The cross sections for electron elastic collisions, electron impact ionization and total electron impact excitation of neon ground state atoms are adopted from [24,25]. The electron impact ionization cross section from the neon metastable level is taken from [26]. The total electron impact excitation cross section from the neon metastable level could not be found in the literature. However, in [27] the corresponding cross sections for argon and krypton are available, and the differences between the cross section values of these two gases are similar to those for electron impact ionization from the metastable levels, presented in [26]. Therefore, it is assumed that the differences between argon and neon are also similar for electron impact ionization and excitation from the metastable levels. Since the cross section for electron impact ionization from the

Fig. 1. (a) Cross sections of the collision processes of electrons, incorporated in the model, for the neon discharge. 1: electron elastic collisions [24,25], 2: electron impact ionization of neon ground state atoms [24], 3: electron impact ionization of neon metastable atoms [26], 4: electron impact ionization of sputtered copper atoms [29], 5: total electron impact excitation of neon ground state atoms [25], 6: total electron impact excitation of neon metastable atoms [26,27], 7: electron impact excitation of neon ground state atoms to the metastable levels [28]. (b) Cross sections of the collision processes of neon ions and fast atoms, incorporated in the model, for the neon discharge. Solid lines: neon ion collisions. 1: ion symmetric charge transfer [30], 2: ion elastic collisions [30], 3: ion impact ionization [31], 4: ion impact excitation to the metastable levels [32]. Dashed lines: neon fast atom collisions, 5: atom elastic collisions [33,34], 6: atom impact ionization [35], 7: atom impact excitation to the metastable levels [36]. (c) Cross sections of the collision processes of electrons, incorporated in the model, for the argon discharge. 1: electron elastic collisions [25,37], 2: electron impact ionization of argon ground state atoms [38], 3: electron impact ionization of argon metastable atoms [26], 4: electron impact ionization of sputtered copper atoms [29], 5: total electron impact excitation of argon ground state atoms [39], 6: total electron impact excitation of argon metastable atoms [27], 7: electron impact excitation of argon ground state atoms to the metastable levels [28]. (d) Cross sections of the collision processes of argon ions and fast atoms, incorporated in the model, for the argon discharge. Solid lines: argon ion collisions. 1: ion symmetric charge transfer [40], 2: ion elastic collisions [40], 3: ion impact ionization [41], 4: ion impact excitation to the metastable levels [41]. Dashed lines: fast argon atom collisions. 5: atom elastic collisions [40], 6: atom impact ionization and excitation to the metastable levels [41].

neon metastable levels is about 75% of the corresponding value for argon [26], the cross section for total electron impact excitation from the neon metastable levels is also assumed to be 75% of the corresponding value for argon. The cross section for electron impact excitation from the neon ground state to the metastable level is taken from [28], and the electron impact ionization cross section of the sputtered copper atoms is obtained from [29].

In Fig. 1b the cross sections for neon ion and atom collisions as a function of the ion and atom energies are illustrated. The solid lines present the neon ion cross sections, whereas the dashed lines apply to the neon atom cross sections. The cross sections for neon ion symmetric charge transfer and elastic collisions are adopted from [30], and the cross sections for neon ion impact ionization and excitation to the metastable levels are taken from [31,32], respectively. The elastic collision cross section for neon atoms is taken from [33] (i.e., deduced from the sequence argon-krypton-xenon as being 80% of the corresponding cross section for argon [34]). Finally, the cross sections for neon atom impact ionization and excitation to the metastable levels are taken from [35,36], respectively. For easy reference, the corresponding cross sections in the argon discharge are illustrated in Fig. 1c (for the electrons) and Fig. 1d (for the argon ions and atoms). Comparison of Figs. 1a and 1c, and Figs. 1b and 1d, indicates that the cross sections for neon are always slightly lower than the corresponding values for argon, which can probably be attributed to the smaller radius of neon atoms, compared to argon.

The other input data necessary for the calculations are summarized in Table 1 for both neon and argon. E_{ioniz} and E_{excit} are the ionization potential and the excitation energy of the lowest (= metastable) energy level, respectively. The numerical values of these quantities, for both neon and argon, are taken from [42]. γ is the ion-induced secondary electron emission coefficient, and the numerical values for neon and argon are calculated with the formula presented in [43]. k_{PI} is the rate coefficient for Penning ionization of the sputtered copper atoms by metastable gas atoms; it is obtained by an empirical formula [44] which was fitted to some experimentally obtained cross sections (i.e., for Ar or Ne + Zn, Cd or Mg [44,45]) in order to arrive at approximate values for Ar or Ne + Cu. k_{CT} is the rate coefficient for asymmetric charge transfer of copper atoms by gas ions. The value for neon was adopted from [46,47], whereas the corresponding value for argon was taken from [48]. These values are poorly known and are therefore subject to large uncertainties. However, the fact that the value for neon is higher than for argon is not unexpected, since copper possesses more ionic energy levels suitable for asymmetric charge transfer with neon than with argon [42,49]. D_+ is the diffusion

Table 1
Input data required for the modelling work, for neon and argon (symbols are explained in the text)

Gas	Neon	Argon
E_{ioniz} (eV)	21.56 [42]	15.76 [42]
E_{excit} (eV)	16.62 [42]	11.55 [42]
γ	0.19 [43]	0.083 [43]
k_{PI} ($cm^3\ s^{-1}$)	2.26×10^{-10} [44]	2.36×10^{-10} [44]
k_{CT} ($cm^3\ s^{-1}$)	2×10^{-9} [46,47]	2×10^{-10} [48]
D_+ ($cm^2\ s^{-1}$)	223 [50]	111 [50]
μ_{+0} ($cm^2\ V^{-1}\ s^{-1}$)	3500 [51]	1460 [51]
a ($cm^{-2}\ V^{-1}$)	1.115×10^{15} [51]	7.36×10^{14} [51]
$D_{Cu,X}$ ($cm^2\ s^{-1}$)	224.5 [50]	144.6 [50]
$\mu_{Cu,X}$ ($cm^2\ s^{-1}\ V^{-1}$)	4873.7 [52]	1837.4 [52]
D_{met} ($cm^2\ s^{-1}$)	150 [53]	54 [53]
k_{recom} ($cm^3\ s^{-1}$)	10^{-11} [54]	10^{-11} [54]
k_{quen} ($cm^3\ s^{-1}$)	2×10^{-7} [55]	2×10^{-7} [55]
k_{met} ($cm^3\ s^{-1}$)	6.4×10^{-10} [55]	6.4×10^{-10} [55]
k_{2B} ($cm^3\ s^{-1}$)	1.55×10^{-15} [56]	2.3×10^{-15} [58]
k_{3B} ($cm^6\ s^{-1}$)	5×10^{-34} [57]	1.4×10^{-32} [58]

coefficient of the gas ions at 1 Torr and 298 K, and is calculated for both neon and argon with a formula presented in [50]. The mobility of neon and argon gas ions, μ_+, is calculated with the formula [51]:

$$\mu_+ = \frac{\mu_{+0}}{\sqrt{1+a\left|\frac{E}{n}\right|}}$$

The parameters μ_{+0} and a, at 1 Torr and 298 K, are adopted from [51] for both neon and argon; E and n represent the electric field strength and the gas density, respectively. $D_{Cu,X}$ is the diffusion coefficient of copper atoms and ions in the neon or argon gas at 1 Torr and 298 K, and is calculated with the formula in [50]. $\mu_{Cu,X}$ is the mobility of copper ions in neon or argon gas at 1 Torr and 298 K, derived from a graph in [52]. D_{met} is the diffusion coefficient of neon and argon metastable atoms at 1 Torr and 298 K, and is taken for both neon and argon from [53]. k_{recom} is the rate coefficient for gas ion-electron radiative recombination, and is obtained from [54]. k_{quen} is the rate coefficient for electron collisional transfer from the metastable levels to the nearby energy levels (electron quenching) and is adopted from [55]. It is taken to be equal for neon and argon, as is suggested in [55]. Also, k_{mel}, the rate coefficient for metastable atom–metastable atom collisions, is assumed to be equal for neon and argon [55]. k_{2B} and k_{3B} are the rate coefficients for two-body and three-body collisions of gas metastable atoms with one or two gas ground state atoms; the numerical values for neon are adopted from [56,57] for k_{2B} and k_{3B}, respectively, and the corresponding values for argon are obtained from [58] for both k_{2B} and k_{3B}.

Finally, the sputtering yield of a copper cathode due to bombardment of neon and argon gas ions and atoms, $Y(E)$, is illustrated as a function of the bombarding particles energies in Fig. 2. It is calculated from an empirical formula [59] depending on the masses and atomic numbers of bombarding and target particles. As expected, the sputtering yield due to argon bombardment is higher (by a factor of about 1.5) than for neon bombarding, because of its higher mass. For comparison, the sputtering yield due to bombardment of copper atoms and ions on a copper cathode (i.e., self-sputtering) is also illustrated in Fig. 2, and it is still higher, because of the higher mass of copper.

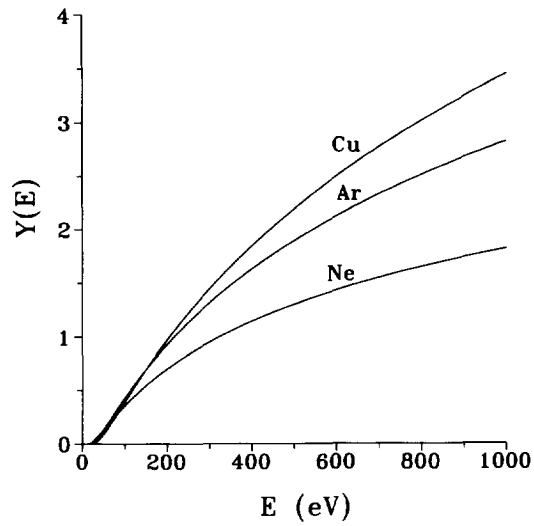

Fig. 2. Sputtering yield of a copper cathode, due to bombardment of copper, argon and neon particles, as a function of the bombarding particles' energies, calculated with the empirical formula of [59].

3. Results and discussion

In [16,19], typical three-dimensional results for the VG9000 glow discharge cell in argon were presented at 1000 V, 75 Pa and 3.4 mA. Therefore, we wanted to perform the calculations for the neon discharge at the same current–voltage values as for argon, to make direct comparisons possible. The electrical current, however, is not used as an input parameter in the models, but is obtained as a self-consistent result from the calculations. Indeed, when pressure, voltage and gas temperature are given, the electrical current follows from the calculated fluxes of the plasma species, and this parameter can be compared with experimental values to check the validity of the models. Therefore, a number of calculations had to be carried out for the neon discharge, to investigate which pressure yielded an electrical current of 3.4 mA at 1000 V. This was found to be the case at a pressure value of 290 Pa.

Hence the pressure in the neon discharge has to be almost a factor of 4 higher than for argon to yield the same electrical characteristics. This is attributed to the slightly lower ionization cross sections of neon as compared to argon (see Figs. 1a, 1b, 1c and 1d), which result in less ionization, i.e., less ions and electrons (current carriers), and, therefore, a lower electrical current. In order to arrive at the same

Table 2
Calculated densities of the different plasma species, at the maximum of their profiles, at 1000 V discharge voltage, 3.4 mA current, a gas temperature of 360 K, and a pressure of 290 Pa (for neon) and 75 Pa (for argon)

Plasma species	Density in neon (cm^{-3})	Density in argon (cm^{-3})
Gas atoms at rest, uniformly distributed	5.8×10^{16}	1.5×10^{16}
Gas ions	5.4×10^{11}	5.5×10^{11}
Slow electrons	5.4×10^{11}	5.5×10^{11}
Fast electrons	3.0×10^{7}	4.0×10^{7}
Gas metastable atoms	7.3×10^{11}	1.1×10^{12}
Sputtered copper atoms	3.1×10^{12}	6.7×10^{12}
Copper ions	1.5×10^{10}	3.4×10^{9}

electrical current, the pressure must be higher, because this gives rise to a higher gas atom density, and hence more probability for collisions. The density of gas atoms, which corresponds to this value of the gas pressure, is indicated in Table 2, together with the density value for the pressure in argon (75 Pa). It should be mentioned that the effect of pressure on the electrical current is not linear. For example, at 290 Pa, the calculated current was about 3.4 mA, whereas the value of the current at 260 Pa amounted to about 2.8 mA. Hence, a variation of about 10% in pressure yielded a variation of about 20% in the calculated current.

It was also observed that small variations in the ionization cross sections could lead to rather large variations in the calculated electrical current. Since the ionization cross sections (especially the ones for neon ion and atom impact ionization) are subject to considerable uncertainties, the factor of 4 increase in the pressure must not be considered as an absolute number. It can also be a factor of 3 or 5, but it is obvious that the pressure in the neon discharge is higher than in the argon discharge for the same current–voltage values.

Fig. 3 shows the neon ion density calculated for 1000 V, 3.4 mA and 290 Pa, for the so-called 'new flat cell' geometry of the VG9000 glow discharge mass spectrometer. A schematic picture of this cell was presented in [16]. The cathode is situated at $z = 0$; the teflon insulator ring (with an aperture diameter of 2 cm), and the front plate at anode potential (with an aperture diameter of 1 cm) are represented by the black rectangles from $z = 0$ cm to $z = 0.05$ cm, and from $z = 0.05$ cm to $z = 0.15$ cm, respectively. The cell walls at the anode potential are situated at $z = 1.05$ cm and at $r = 1.25$ and $r = -1.25$ cm. The neon ion density is low and is more or less constant ($1-2 \times 10^{10}$ cm^{-3}) in the region close to the cathode (i.e., the cathode dark space, CDS), and reaches a maximum of about 5.4×10^{11} cm^{-3} in the middle of the discharge (in the negative glow, NG). Both the shape and the absolute values of this density profile resemble very closely the argon ion density profile at 1000 V, 3.4 mA and 75 Pa, which was presented in Fig. 4a of [16].

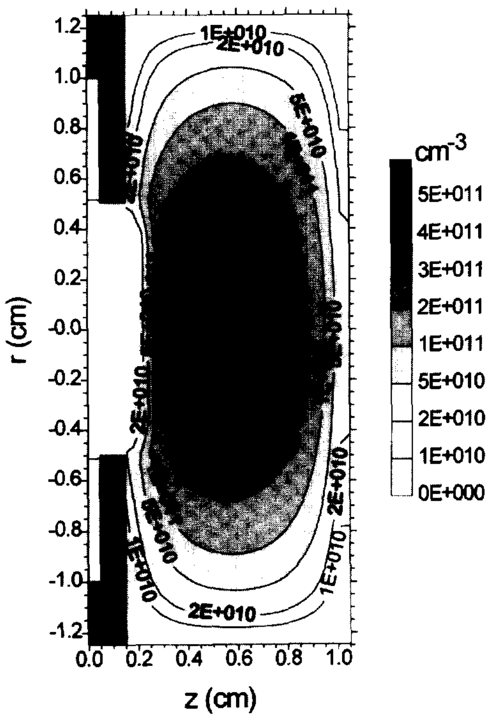

Fig. 3. Calculated number density profile of the neon ions (VG9000 glow discharge cell, 1000 V, 3.4 mA, 290 Pa, neon discharge with copper cathode).

The slow electron density profile (not shown here) is almost identical to the neon ion density profile, except that it is zero in the CDS and at the cell walls. This gives rise to a net positive space charge in the CDS and nearly charge neutrality in the NG. This situation is very similar to the argon discharge [16]. Also the fast electron density profile resembles closely the corresponding fast electron density profile in argon (Fig. 4c of [16]), and is therefore not shown here. The value at the maximum is only slightly lower than for the argon discharge. The densities of the plasma species at the maximum of their profiles, for both the neon and the argon discharge, are indicated in Table 2. It appears that at the same electrical discharge conditions, the gas ion and electron densities are quite similar for both the neon and the argon discharge. This is as expected since the densities of the plasma species are closely correlated to the fluxes, and since the gas ions and electrons are the dominant current carriers, comparable densities are indeed expected at the same electrical current.

In Fig. 4, the neon metastable atom density profile is illustrated. The density reaches a pronounced maximum close to the cathode, it decreases further in the discharge and reaches a second, less distinct maximum at about 0.8 cm from the cathode. This density profile is similar to the corresponding argon metastable atom density profile, which was depicted in [19] (Fig. 2). The values at the maxima of the profiles are given in Table 2; the neon metastable atom density appears to be only slightly lower than the argon metastable atom density. It was indeed found that the same production and loss processes played a dominant role for both the neon and argon metastable atoms. The relative contributions of the different production and loss processes, integrated over the total discharge region, are presented in Table 3.

The main production process in both cases appears to be fast gas (neon or argon) atom impact excitation to the metastable levels. This process, plus fast gas ion impact excitation, which plays also a non-negligible role, is only important close to the cathode; the gas atoms and ions reach there, indeed, their highest energies (see below), and the cross sections of these processes increase with the impact energies (see Fig. 1b and 1d). This explains the pronounced maximum in the metastable density profiles close to the cathode. The contribution of electron impact excitation to the metastable levels also plays a significant role. This process is especially important in the beginning of the NG (i.e., at about 0.3–0.4 cm from the cathode). The fourth production process incorporated in the models, i.e., electron–ion radiative recombination was found to be negligible for both argon and neon.

Diffusion and subsequent deexcitation at the cell walls is the most important loss process for both the neon and argon metastable atoms, as shown in Table 3. This process is especially important close to the cathode, in order to spread out the metastable atom

Table 3
Calculated relative contributions of the different production and loss processes for the gas metastable atoms, at 1000 V discharge voltage, 3.4 mA current, a gas temperature of 360 K, and a pressure of 290 Pa (for neon) and 75 Pa (for argon)

Production processes	Contribution in neon (%)	Contribution in argon (%)
Electron impact excitation	19	13
Gas ion impact excitation	12	17
Gas atom impact excitation	69	70
Electron–ion recombination	0.01	0.01
Loss processes		
Diffusion + deexcitation at walls	78	82
Electron quenching	17	11
Penning ionization of copper	2.5	3.7
Metastable–metastable collisions	1.7	3.0
Electron impact excit. from metast.	0.2	0.3
Electron impact ioniz. from metast.	0.01	0.02
Two-body collisions with gas atoms	0.3	0.1
Three-body collisions with gas atoms	0.01	0.01

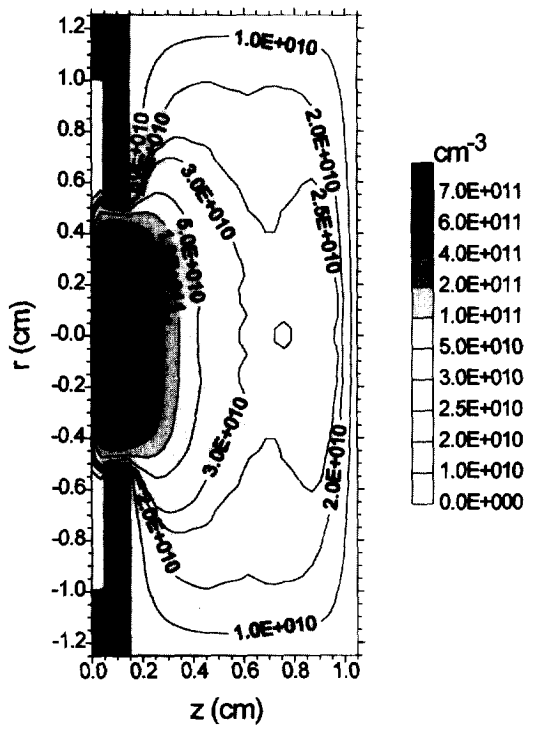

Fig. 4. Calculated number density profile of the neon metastable atoms (VG9000 glow discharge cell, 1000 V, 3.4 mA, 290 Pa, neon discharge with copper cathode).

number density, created there by gas atom and ion impact excitation. Collisional transfer to the nearby energy levels by collisions with slow electrons (called electron quenching) is also a significant loss process; it occurs mainly in the NG, where the slow electron density profile, in both neon and argon, is at its maximum. Beside these two major loss processes, Penning ionization of the sputtered copper atoms and metastable atom–metastable atom collisions play a non-negligible role too. The other four loss processes incorporated in the model, i.e., electron impact excitation and ionization from the metastable levels, and two-body and three-body collisions with gas atoms, were found to be unimportant, for both neon and argon. It should be mentioned that the numerical data of the relative contributions of the production and loss processes have to be considered with caution, since the rate constants and cross sections, especially the ones for ion and atom impact excitation, are subject to unknown uncertainties. Nevertheless, the data in Table 3 can give a qualitative idea about the relative importances of the different production and loss processes of the metastable atoms.

In Fig. 5, the sputtered copper atom density profile in the neon discharge, at 1000 V, 3.4 mA and 290 Pa, is depicted. The density reaches a maximum at 1–2 mm from the cathode and decreases further in the discharge. The shape of the profile is similar to the corresponding copper atom density profile in the argon discharge (presented in Fig. 5 of [19]), but the absolute value is a factor of 2–3 lower, as also indicated in Table 2. This is attributed to the lower sputtering yield in neon than in argon, due to its lower atomic mass (see Fig. 2).

We have calculated explicitly the sputtering rate (or erosion rate) of copper atoms in the neon and argon discharge, by [23]:

$$(ER)_1 = J_{\text{sput, net, 1}} \frac{M}{N_A \rho} \text{ and } (ER)_2 = J_{\text{sput, net, 2}} \frac{M}{N_A}$$

$(ER)_1$ and $(ER)_2$ both represent the erosion rates, in cm s^{-1} and in g s^{-1}, respectively. $J_{\text{sput,net,1}}$ and $J_{\text{sput,net,2}}$

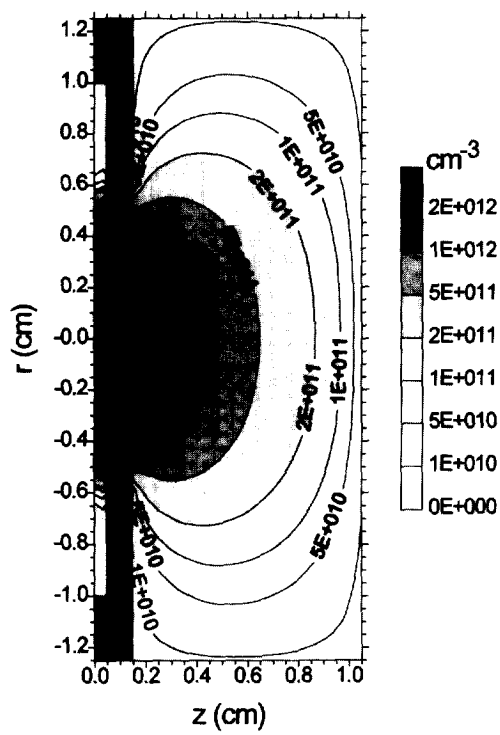

Fig. 5. Calculated number density profile of the sputtered copper atoms (VG9000 glow discharge cell, 1000 V, 3.4 mA, 290 Pa, neon discharge with copper cathode).

are the net fluxes of sputtered copper atoms (in $cm^{-2}\ s^{-1}$ and in s^{-1}, respectively), which are obtained from the total flux of sputtered atoms minus the flux of redeposited copper atoms. The latter reaches a rather high value for both neon and argon, as shown in Table 4; about 63% of the flux of sputtered copper atoms is redeposited again onto the cathode in the neon discharge, and about 57% diffuses back towards the cathode in the argon discharge. The slightly higher value of the redeposition flux calculated for neon is due to the higher pressure in neon, which ensures that the sputtered copper atoms cannot diffuse very far in the discharge and have more chance to deposit again onto the cathode. M and ρ are the atomic weight ($g\ mol^{-1}$) and density of the sample material (ρ_{Cu} = 8.92 $g\ cm^{-3}$ [60]), and N_A is Avogadro's number. The erosion rates, calculated both in depth and in weight per unit time, are presented in Table 4. These values are in reasonable agreement with typical values obtained experimentally in GDMS [61], which is a validation of our model. It appears that the erosion rates in the neon discharge are a factor of 2–3 lower than the corresponding values in the argon discharge, as expected from the lower sputtering yield.

Fig. 6 illustrates the copper ion density profile in the neon discharge, at 1000 V, 3.4 mA and 290 Pa. This profile has nearly the same shape as the argon ion density profile, i.e., it is low and rather constant in the CDS and reaches a maximum in the middle of the NG. This shape is again similar to the copper ion density profile calculated for the argon discharge (Fig. 8 in [19]); however, the absolute value in neon is a factor of 4 higher, as shown in Table 2. Since the sputtered copper atom density in neon was found to be lower than in argon (see above), this indicates that the ionization efficiency of copper is higher in the neon glow discharge. It was found that the efficiencies of electron impact ionization and Penning ionization by metastable gas atoms were comparable in neon and argon, but that asymmetric charge transfer with gas ions was clearly more important in the neon discharge. This follows indeed from the rate coefficient of this process, which was found in the literature to be an order of magnitude higher with neon than with argon (see Table 1).

The relative contributions of electron impact ionization, Penning ionization and asymmetric charge transfer to the ionization of copper atoms, calculated for both the neon and the argon discharge, are summarized in Table 4. Since the absolute efficiencies of electron impact ionization and Penning ionization are comparable in neon and argon, and the absolute efficiency of asymmetric charge transfer is clearly higher in neon than in argon, it follows that the relative contribution of the latter process to the ionization of copper is significantly higher for neon than for argon.

Owing to the higher efficiency of asymmetric charge transfer with neon, it can also be expected that the calculated ionization degree of copper is higher in the neon discharge than in the argon discharge. This can indeed be noticed from Table 4 (i.e., the ionization degree of copper is about 0.6% in neon and about 0.1% in argon). When we compare these values with the calculated ionization degrees for neon and for argon (i.e., the ionization degree of neon

Table 4
Calculated quantities concerning the sputtered material, at 1000 V discharge voltage, 3.4 mA current, a gas temperature of 360 K, and a pressure of 290 Pa (for neon) and 75 Pa (for argon)

Calculated quantities	In neon	In argon
Redeposition of sputtered atoms	63%	57%
Erosion rate	3.2 $\mu m\ h^{-1}$	8 $\mu m\ h^{-1}$
Erosion rate	0.73 $\mu g\ s^{-1}$	1.7 $\mu g\ s^{-1}$
Contribution of electron impact ionization of copper	1%	4%
Contribution of Penning ionization of copper	14%	59%
Contribution of asymmetric charge transfer of copper	85%	37%
Ionization degree of copper	0.6%	0.1%
Ionization degree of the gas atoms	8×10^{-6}	3×10^{-5}
Ratio of copper atom to gas atom density	5.3×10^{-5}	4.5×10^{-4}
Ratio of copper ion to gas ion density	2.8%	0.62%

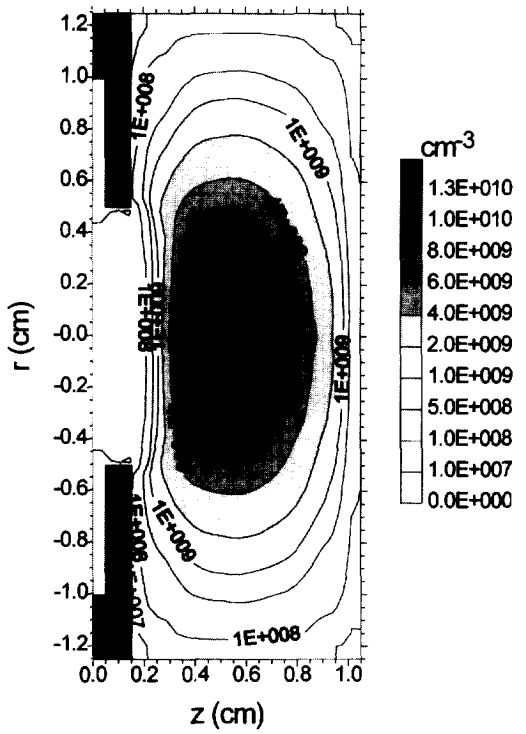

Fig. 6. Calculated number density profile of the copper ions (VG9000 glow discharge cell, 1000 V, 3.4 mA, 290 Pa, neon discharge with copper cathode).

is about 8×10^{-6} and that of argon is about 3×10^{-5}), we can conclude that, in both environments, the sputtered copper atoms are clearly more efficiently ionized than the gas (neon and argon) atoms, due to the possibility of Penning ionization and asymmetric charge transfer, ionization processes that are excluded for neon and argon.

From the densities at the maximum of their profiles, presented in Table 2, the ratio of sputtered copper atoms to gas atoms and of copper ions to gas ions in the glow discharge can be deduced. These values are given in Table 4. The copper atom density is about 4–5 orders of magnitude lower than the gas atom densities, but the ratios of copper ion to gas ion densities were calculated to be more or less in the percent order. This indicates again that the sputtered copper atoms are more efficiently ionized than the gas atoms.

It is important to mention here that the rate constants of asymmetric charge transfer, both for Ne–Cu and Ar–Cu, are subject to unknown uncertainties, and the calculated relative contributions of different ionization processes for copper, the ionization degree of copper and the ratios of copper ion to gas ion densities have, therefore, to be considered with caution. Moreover, the present results may not be generalized to other elements: in the case of copper, asymmetric charge transfer is more efficient with neon than with argon, due to the availability of suitable energy levels [49], but this is not necessarily true for other elements [62].

The densities of the charged plasma species give rise to certain potential and electric field distributions, calculated self-consistently in the models by using the Poisson equation. Since the densities of the gas ions and slow electrons (i.e. the two dominant charged species in the present discharges) are of comparable magnitude in both the neon and the argon discharge (see above), it is not surprising that the potential and electric field distributions in neon and in argon are

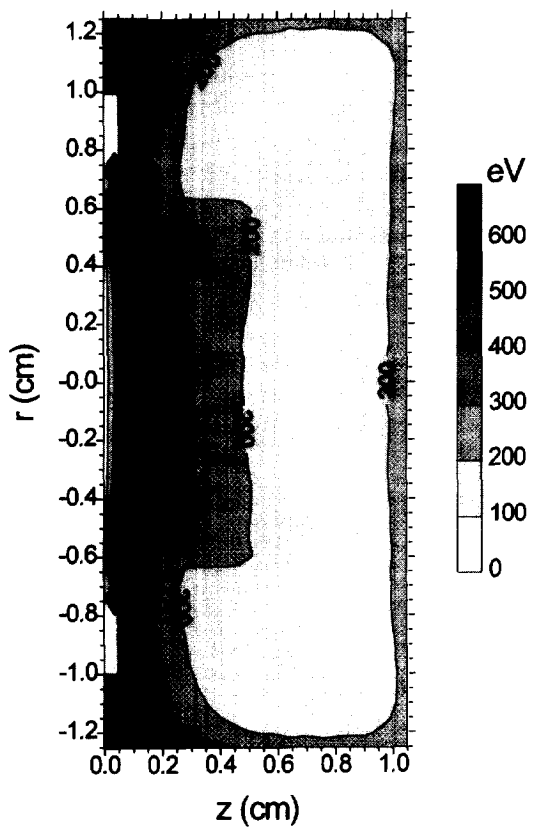

Fig. 7. Calculated mean energy distribution of the fast electrons throughout the discharge (VG9000 glow discharge cell, 1000 V, 3.4 mA, 290 Pa, neon discharge with copper cathode).

nearly equal as well. Therefore, these distributions in neon are not presented here, but we refer to the corresponding distributions for argon (shown in Fig. 5, Fig. 6a and Fig. 6b of [16]).

The last topic in the present comparison between neon and argon concerns the energies of the plasma species. Fig. 7 presents the electron mean energy distribution throughout the neon discharge. The electrons start at the cathode with low energies. On their way towards the anode, they gain energy from the electric field in the CDS, so that their mean energy increases. On the other hand, they also lose energy by collisions. Therefore, at the end of the CDS, the mean energy is lower than the total discharge voltage, but it is still about 560 eV. It is interesting to mention here that the interface between CDS and NG is defined in our models as the position where the potential goes through zero, which was calculated to be at about 0.24 cm from the cathode. In the NG, the electrons do not gain much energy from the electric field, which is very low in this region, but they mainly lose energy due to collisions. Therefore, the mean energy of the electrons decreases on their further way towards the anode. However, at the anode backplate (i.e., at 1.05 cm from the cathode), the mean electron energy was calculated to be still about 200 eV, as can be seen in Fig. 7. When comparing Fig. 7 with the corresponding electron mean energy distribution in the argon discharge (i.e., Fig. 7a of [16]), we can conclude that the mean energy of the electrons at the end of the CDS (i.e., the maximum of the mean energy that they can reach in the discharge) is more or less comparable for both the neon and the argon discharge (see also Table 5), but the overall mean energy of the electrons in the NG is slightly lower in the neon discharge. This is attributed to the higher pressure in the neon discharge. Indeed, this gives rise to a higher gas atom number density, and, hence, to a larger number of collisions (in spite of the fact that the cross sections in neon are slightly lower), and, therefore, to more energy loss.

The same effect is found in the mean energies of the other plasma species (i.e., the gas ions and fast atoms, and the copper ions). These species are assumed to be thermalized in the NG, but their mean energy increases in the CDS on their way towards the cathode. Their maximum mean energy is therefore observed at the cathode. From Table 5, where the maximum mean energies of these species in both gases are given, it can indeed be seen that the energies are definitely lower in the neon discharge, due to the higher pressure, which gives rise to more collisions and hence more energy losses. The maximum gas ion mean energy is clearly lower than the maximum electron mean energy. Since both species gain the same amount of energy from the electric field, this indicates that the gas ions lose their energy more efficiently and more frequently in collisions than the electrons. Indeed the symmetric charge transfer collisions (which are the dominant collision processes of the gas ions) have larger cross sections and are more efficient in lowering the ion energies (i.e., the gas ions start again from rest after such a collision) than the electron collision processes (excitation and ionization). The maximum mean energies of the fast gas atoms are still lower, since these species are created from the gas ions, but they cannot gain energy from the electric field, they can only lose their energy by

Table 5
Calculated mean energies of the plasma species, at the maximum of the distributions (i.e., for the electrons at the end of the CDS, and for the ions and fast atoms at the cathode; all values are taken at the cell axis), and calculated contributions to sputtering of the plasma species bombarding the cathode, at 1000 V discharge voltage, 3.4 mA current, a gas temperature of 360 K, and a pressure of 290 Pa (for neon) and 75 Pa (for argon)

Calculated quantities	In neon	In argon
Max. electron mean energy (at end of CDS)	560 eV	600 eV
Max. gas ion mean energy (at cathode)	60 eV	135 eV
Max. fast gas atom mean energy (at cathode)	14 eV	33 eV
Max. copper ion mean energy (at cathode)	670 eV	730 eV
Contribution of fast gas atoms to cathode sputtering	73%	72%
Contribution of gas ions to cathode sputtering	21%	26%
Contribution of copper ions to cathode sputtering	6%	2%

collisions. The maximum mean energy of the copper ions, on the other hand, is much higher. Indeed, the copper ions gain energy from the electric field in the CDS and they do not lose this energy very efficiently by collisions.

Since the energy of the copper ions bombarding the cathode is considerably higher than the energies of the gas ions and atoms, it can be expected that their contribution to the sputtering processes at the cathode is not negligible, in spite of their lower flux. The calculated relative contributions to sputtering of the fast gas atoms, gas ions and copper ions are presented in Table 5. The fast gas atoms appear to play the most significant role in sputtering, in both neon and argon; the gas ions take second place, but the contribution of the copper ions (i.e., self-sputtering) is not negligible. The role of self-sputtering was found to be somewhat higher in neon than in argon, due to the higher copper ion to neon ion ratio (see Table 4), and also because neon is not as efficient at sputtering as argon and copper (see Fig. 2).

4. Conclusion

The set of three-dimensional models, which was developed earlier for a direct-current glow discharge in argon, is applied to a neon glow discharge in the present paper, and the differences between these two discharge gases are investigated. The major difference is that the neon discharge has to be operated at a higher pressure, in order to arrive at similar electrical conditions (voltage and current) as those for the argon discharge. At 1000 V and 3.4 mA, the argon gas pressure was found to be 75 Pa, whereas the pressure in neon was calculated to be 290 Pa, i.e., a factor of about 4 higher.

Apart from that, when both the neon and the argon discharge are operated at the same voltage and electrical current, they exhibit a quite similar behaviour. The densities of gas ions, fast and slow electrons, and gas metastable atoms, and the relative contributions of the different production and loss processes for the metastables, are more or less similar for both neon and argon. Also the potential and electric field distributions in neon and in argon are comparable. The erosion rate and the sputtered copper atom density are a factor of 2–3 lower in neon than in argon, since neon is not as efficient at sputtering due to its lower atomic mass. However, the copper ion density appears to be a factor of 4 higher in neon than in argon; hence, also, the ionization degree of copper, the ratio of copper ion to gas ion densities, and the role of copper ions in the discharge (i.e., with respect to sputtering) were found to be slightly higher in neon. This is attributed to the rate coefficient of asymmetric charge transfer, which was found in the literature to be one order of magnitude higher for Cu–Ne than for Ar–Ne. However, due to the uncertainties in the rate coefficients of asymmetric charge transfer, these results have to be considered with caution. Moreover, the rate coefficients are element-specific, and the results can, therefore, not be generalized to other elements. Finally, due to the higher pressure in neon, the plasma species will undergo more collisions with the gas atoms, and are, therefore, characterized by somewhat lower energies.

In general, although some of the results may not yet be considered quantitative, due to uncertainties in some cross sections, the present study can yield a better qualitative understanding about the differences and similarities of neon and argon as discharge gases.

Acknowledgements

A. Bogaerts is indebted to the Belgian National Fund for Scientific Research (NFWO) for financial support. The authors also acknowledge financial support from the Federal Services for Scientific, Technical and Cultural Affairs (DWTC/SSTC) of the Prime Minister's Office through IUAP-III (Conv. 49). Finally, they wish to thank A.V. Phelps for supplying references about cross sections for neon atom and ion collisions.

References

[1] R. K. Marcus, Glow Discharge Spectroscopies, Plenum Press, New York, 1993.
[2] B. Chapman, Glow Discharge Processes, Wiley, New York, 1980.
[3] D.C. Gerstenberger, R. Solanki and G.J. Collins, IEEE Journal of Quant. Electron., 16 (1980) 820.
[4] E.W. Eckstein, J.W. Coburn and E. Kay, Int. J. Mass Spectrom. Ion Phys., 17 (1975) 129.

[5] K.C. Smyth, B.L. Bentz, C.G. Bruhn and W.W. Harrison, J. Amer. Chem. Soc., 101 (1979) 797.
[6] K. Wagatsuma and K. Hirokawa, Anal. Chem., 57 (1985) 2901.
[7] C.E. Light and E.B.M. Steers, Analyst, 110 (1985) 439.
[8] N. Jakubowski and D. Stüwer, Fres. Z. Anal. Chem., 335 (1989) 680.
[9] X.L. Han, V. Wisehart, S.E. Conner, M.-C. Su and D.L. Monts, Contrib. Plasma Phys., 34 (1995) 439.
[10] A. Bogaerts, A. Quentmeier, N. Jakubowski and R. Gijbels, Spectrochim. Acta Part B, 50 (1995) 1337.
[11] J.J. Giglio and J.A. Caruso, Appl. Spectrosc., 49 (1995) 900.
[12] F. Leis and E.B.M. Steers, Fres. J. Anal. Chem., 355 (1996) 873.
[13] R.E. Valiga, D.C. Duckworth and D.H. Smith, Rapid Comm. Mass Spectrom., 10 (1996) 305.
[14] A. Bogaerts, M. van Straaten and R. Gijbels, Spectrochim. Acta Part B, 50 (1995) 179.
[15] A. Bogaerts, R. Gijbels and W.J. Goedheer, J. Appl. Phys., 78 (1995) 2233.
[16] A. Bogaerts, R. Gijbels and W.J. Goedheer, Anal. Chem., 68 (1996) 2296.
[17] A. Bogaerts and R. Gijbels, J. Appl. Phys., 78 (1995) 6427.
[18] A. Bogaerts and R. Gijbels, Phys. Rev. A, 52 (1995) 3743.
[19] A. Bogaerts and R. Gijbels, Anal. Chem., 68 (1996) 2676.
[20] A. Bogaerts, M. van Straaten and R. Gijbels, J. Appl. Phys., 77 (1995) 1868.
[21] A. Bogaerts and R. Gijbels, J. Appl. Phys., 79 (1996) 1279.
[22] A. Bogaerts and R. Gijbels, Fres. J. Anal. Chem., 355 (1996) 853.
[23] A. Bogaerts, Ph.D. Dissertation, University of Antwerp, 1996.
[24] F.J. de Hoog and J.G.A. Holscher, Physica, 54 (1971) 529.
[25] F.J. de Heer, R.H.J. Jansen and W. van der Kaay, J. Phys. B., 12 (1979) 979.
[26] H.A. Hyman, Phys. Rev. A., 20 (1979) 855.
[27] H.A. Hyman, Phys. Rev. A., 18 (1978) 441.
[28] N.J. Mason and W.R. Newell, J. Phys. B., 20 (1987) 1357.
[29] L. Vriens, Phys. Lett., 8 (1964) 260.
[30] W.H. Cramer, J. Chem. Phys., 28 (1958) 688.
[31] H.B. Gilbody et al., Proc. Roy. Soc., A240 (1957) 382.
[32] R.C. Isler and L.E. Murray, Phys. Rev. A. 13 (1976) 2087.
[33] R.S. Robinson, J. Vac. Sci. Technol., 16 (1979) 185.
[34] A.V. Phelps, private communication.
[35] R.C. Amme, Phys. Rev., 177 (1969) 230.
[36] V. Kempter, F. Veith and L. Zehnle, J. Phys. B, 8 (1975) 2835.
[37] W.C. Fon, K.A. Berrington, P.G. Burke and A. Hibbert, J. Phys. B., 16 (1983) 307.
[38] R.J. Carman, J. Phys. D., 22 (1989) 55.
[39] E. Eggarter, J. Chem. Phys., 62 (1975) 833.
[40] A.V. Phelps, J. Appl. Phys., 76 (1994) 747.
[41] A.V. Phelps, J. Phys. Chem. Ref. Data, 20 (1991) 557.
[42] C.E. Moore, Atomic Energy Levels, Volume I–III, Nat. Stand. Ref. Data Ser., Nat. Bur. Stand. (US), 1971.
[43] H. Oechsner, Phys. Rev. B., 17 (1978) 1052.
[44] L.A. Riseberg, W.F. Parks and L.D. Schearer, Phys. Rev. A, 8 (1973) 1962.
[45] S. Inaba, T. Goto and S. Hattori, J. Phys. Soc. Jpn., 52 (1983) 1164.
[46] B.E. Warner, K.B. Persson and G.J. Collins, J. Appl. Phys., 50 (1979) 5694.
[47] E.M. van Veldhuizen and F.J. de Hoog, J. Phys. D, 17 (1984) 953.
[48] S.C. Rae and R.C. Tobin, J. Appl. Phys., 64 (1988) 1418.
[49] E.B.M. Steers and R.J. Fielding, J. Anal. Atom. Spectrom., 2 (1987) 239.
[50] J.O. Hirschfelder, C.F. Curtiss and R.B. Bird, Molecular Theory of Gases and Liquids, Wiley, New York, 1964.
[51] L.S. Frost, Phys. Rev., 105 (1957) 354.
[52] E.W. McDaniel, Collision Phenomena in Ionized Gases, Wiley, New York, 1964.
[53] A.V. Phelps and J.P. Molnar, Phys. Rev., 89 (1953) 1202.
[54] M.A. Biondi, Phys. Rev., 129 (1963) 1181.
[55] C.M. Ferreira, J. Loureiro and A. Ricard, J. Appl. Phys., 57 (1985) 82.
[56] K.A. Hardy and J.W. Sheldon, J. Appl. Phys., 53 (1982) 8532.
[57] A.V. Phelps, Phys. Rev., 114 (1959) 1011.
[58] K. Tachibani, Phys. Rev. A., 34 (1986) 1007.
[59] N. Matsunami, Y. Yamamura, Y. Itikawa, N. Itoh, Y. Kazumata, S. Miyagawa, K. Morita, R. Shimizu and H. Tawara, Atom. Data and Nucl. Data Tables, 31 (1984) 1.
[60] R.C. Weast and M.J. Astle, CRC Handbook of Chemistry and Physics, 63rd Ed., CRC Press, Boca Raton, 1982–1983.
[61] C. Jonkers, Ph.D. Dissertation, University of Antwerp, Antwerp, 1995.
[62] J. Robben, B.Sc. Dissertation, University of Antwerp, Antwerp, 1996.